ELSEVIER

Polymer 43 (2002) 2959–2967

polymer

www.elsevier.com/locate/polymer

Synthesis, characterization and properties of tetramethyl stilbene-based epoxy resins for electronic encapsulation

Ching Hsuan Lin[a], Jung Min Huang[b], Chun-Shan Wang[b,*]

[a]*Department of Applied Fiber Style, Kun Shan University of Technology, Tainan, Taiwan, ROC*
[b]*Department of Chemical Engineering, National Cheng Kung University, Tainan 701, Taiwan, ROC*

Received 29 October 2001; received in revised form 15 January 2002; accepted 22 January 2002

Abstract

Two novel tetramethyl stilbene-based novolac (**II** and **IV**) were synthesized from 2,6-dimethyl phenol and chloroacetaldehyde dimethylacetal or chloroacetone, and then the resulted novolacs were epoxidized to tetramethyl stilbene-based epoxy resins (**III** and **V**). The proposed structures were confirmed by FTIR, elemental analysis, mass spectra, NMR spectra and epoxy equivalent weight titration. The synthesized tetramethyl stilbene-based epoxy resins were cured with 4,4-diaminodiphenyl methane (DDM) and 4,4-diaminodiphenyl sulfone (DDS). Thermal properties of cured epoxy resins were studied using dynamic mechanical analyzer, differential scanning calorimeter, thermal expansion analyzer and thermal gravimetric analyzer (TGA). These data were compared with that of the commercial tetramethyl biphenol (TMBP) epoxy system. According to the experimental data, the order of T_g for cured epoxy system is **III** > TMBP > **V**. The order of moisture absorption for cured epoxy system is **V** < **III** < TMBP. According to TGA, the 5% degradation temperatures in nitrogen atmosphere were in the range 370–377 and 397–412 °C for DDM and DDS curing systems, respectively. In air atmosphere, the 5% degradation temperatures were in the range 372–385 and 410–411 °C for DDM and DDS curing systems, respectively. The CTE is in inverse order with T_g, therefore, **III**/DDS < TMBP/DDS < **V**/DDS. © 2002 Elsevier Science Ltd. All rights reserved.

Keywords: Stilbene; Tetramethyl; 2,6-Dimethyl phenol

1. Introduction

Encapsulation (packaging) is the last step of integrated circuits fabrication. Encapsulating materials must protect components from chemicals and mechanical stress, ensure a good electrical insulation, and offer a good thermal conductivity. Owing to the lower cost and easier processing, over 90% of encapsulation materials are polymers. Among these polymers, epoxy resins loaded with 70–90% silica micro-particles were most widely used. Currently, glycidyl ether of *o*-cresol novolac epoxy (CNE) is the most widely used encapsulating material. However, the high moisture absorption and melt viscosity of the resin have limited its usage in ultra large-scale integrated circuits (ULSI). An epoxy with low viscosity can be loaded with higher amount of silica micro-particles, and thus reduce the moisture absorption, internal stress and increase encasulant's conductivity. However, low viscosity epoxy resins often are low functionality with high epoxy equivalent weight, and thus cause low heat resistance compared with CNE.

Mesogene-containing epoxy, such as stilbene-based [1–3], phenylbenzoate-based [4–5], biphenolether-based [6–8] and so on, when cured at proper condition, can enhance the thermal and mechanical properties of cured epoxy. Furthermore, due to the hydrophobic properties of methyl group, an epoxy with high methyl group substitution will reduce its moisture absorption [9–10]. In this paper, combining the mesogene and methyl effect, two tetramethyl stilbene-based epoxy (**III** and **V**) were synthesized from the epoxidation of 2,6-dimethyl phenol-chloroacetaldehyde dimethylacetal novolac (**II**) or 2,6-dimethyl phenol-chloroacetone novolacs (**IV**). The structure of novolac (**II** and **IV**) and epoxy (**III** and **V**) were characterized by elemental analysis, IR spectra, mass spectra, NMR spectra and epoxy equivalent weight (EEW) titration. The resulted epoxy resins were cured and their properties were evaluated by differential scanning calorimeter (DSC), thermal gravimetric analyzer (TGA), dynamic mechanical analyzer (DMA) and thermal expansion analyzer (TMA). These data were compared with that of commercial tetramethyl biphenol (TMBP) epoxy system.

* Corresponding author. Tel.: +886-6275-7575; fax: +886-6234-4496.
E-mail address: cswang@mail.ncku.edu.tw (C.-S. Wang).

0032-3861/02/$ - see front matter © 2002 Elsevier Science Ltd. All rights reserved.
PII: S0032-3861(02)00090-3

2. Materials

Chloroacetaldehyde dimethylacetal was purchased from Fluka, and 2,6-dimethylphenol, 4,4-diaminodiphenyl methane, 4,4′-diaminodiphenyl sulfone, chloroacetone, acetic acid and epichlorohydrin were purchased from Acros. TMBP, YX4000H was obtained from Shell. All solvents used were commercial products (HPLC grade) and used without further purification.

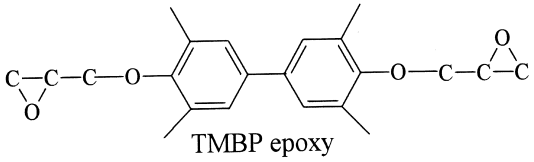

TMBP epoxy

3. Characterization

DSC scans were obtained from samples of about 6 mg in a nitrogen atmosphere at a heating rate of 20 °C/min using a Perkin–Elmer DSC 7. TGA was performed with a Perkin–Elmer TGA 7 at a heating rate of 20 °C/min under nitrogen or air from 60 to 800 °C. DMA was carried out with a Perkin–Elmer DMA 7e. The storage modulus E' and tan δ were determined as the sample was subjected to temperature scan mode at a programmed heating rate of 10 °C/min from ambient to 300 °C at a frequency of 1 Hz and an amplitude of 6 μm. A sample 15 mm in length, 10 mm in width and approximately 1.5 mm in thickness was used. The test method was performed by three point bending mode with a tension ratio at 110%. TMA was carried out with a Perkin–Elmer DMA 7e with a TMA mode. The sample was subjected to temperature scan mode at a programmed heating rate of 10 °C/min from ambient to 300 °C. EEWs of the epoxy resins were determined by the $HClO_4$/potentiometric titration method. Moisture absorption was tested as follows. Samples with $1 \times 1\ cm^2$ and 0.1 cm thickness was dried under vacuum at 120 °C until moisture had been expelled. After cooling down to room temperature, the sample was weighed and then placed in 100 °C water for 24 h and weighed. The moisture absorption was calculated as percent weight gain $= (W/W_0 - 1) \times 100$, where W is the weight of sample after placing in 100 °C water for 24 h and W_0 is the weight of sample before placing in water.

*3.1. Synthesis of 1,1-bis(4-hydroxy-3,5-dimethylphenyl)-2-chloroethane (**I**) [11,12]*

To a four-neck round-bottom flask equipped with a nitrogen inlet, heating mantle, stirrer, thermocouple and temperature controller, 244.4 g (2 mol) of 2,6-dimethyl phenol, 124.57 g (1 mol) of chloroacetaldehyde dimethyl-acetal, and 375 g of acetic acid were added. The reaction

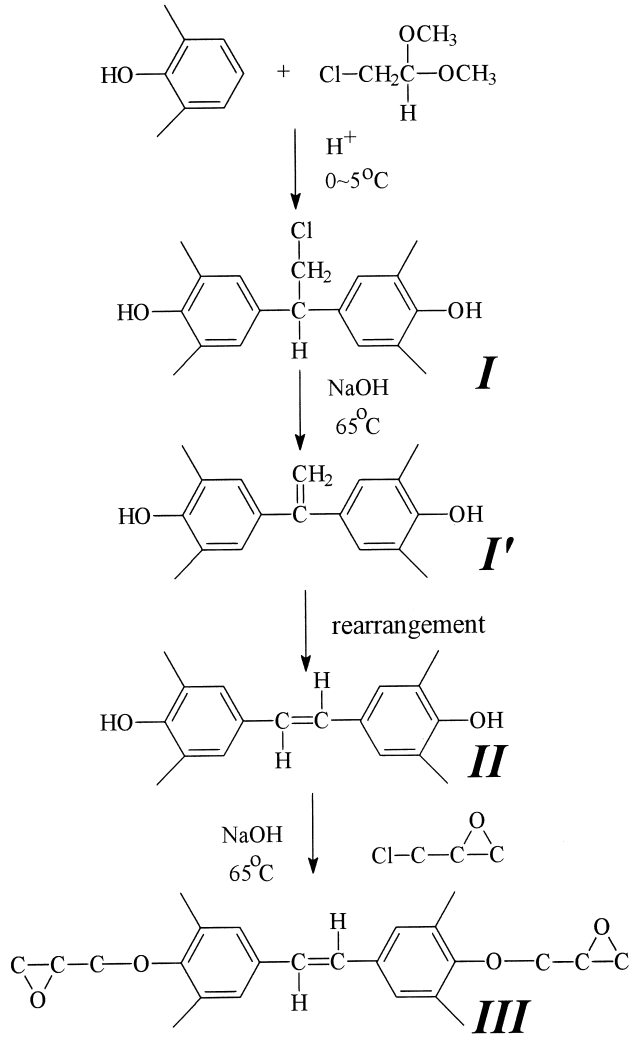

Scheme 1. The reaction equation and structure of **I**–**III**.

mixture was gradually cooled to 5 °C and then a mixture (122 g, 1.2 mol, H_2SO_4 in 84 g acetic acid) was added gradually in 3 h. After that, the reaction mixture was warmed to room temperature and maintained at room temperature for another 24 h. After the reaction was completed, the reaction temperature was cooled to 5 °C again. The reaction mixture was filtered and the white precipitate was washed with water. After drying, the product was recrystallized from xylene. Elemental analyses for $C_{18}H_{21}O_2Cl$: C = 70.93%, H = 6.89% (theoretically) and C = 70.85%, H = 6.67% (experimentally). IR absorption at 680 cm^{-1} (C–Cl), 875 cm^{-1} (aromatic, C–H), 1488 cm^{-1} (aromatic, C=C), 2926 cm^{-1} ($-CH_3$) and 3066–3699 cm^{-1} (–OH). The reaction equation was shown in Scheme 1.

*3.2. Synthesis of 4,4′-dihydroxy-3,3′,5,5′-tetramethyl stilbene (**II**) [11,12]*

To a four-neck round-bottom flask equipped with a

nitrogen inlet, heating mantle, stirrer, thermocouple and temperature controller, **I** of 255.6 g (0.84 mol) and methanol of 451.2 g were added. The reaction mixture was controlled at 30 °C and then 310.7 g of 20 wt% $NaOH_{(aq)}$ was added gradually for 1 h. After that, the mixture was reacted at reflux temperature for 3 h. When the reaction was completed, 37.5 g HCl was added to neutralize excess NaOH. The solution was concentrated and poured into large amount of water. The precipitate was filtered, dried and recrystallized from chlorobenzene. Elemental analyses for $C_{18}H_{20}O_2$: C = 80.59%, H = 7.46%, O = 11.95% (theoretically) and C = 80.49%, H = 7.42%, O = 12.09% (experimentally). IR absorption at 948 cm^{-1} (*trans*, –HC=CH–), 1632 cm^{-1} (C=C), 2918 cm^{-1} ($-CH_3$) and 3066–3755 cm^{-1} (OH). The reaction equation was shown in Scheme 1.

*3.3. Synthesis of 4,4′-bis(2,3-epoxypropoxy)-3,3′,5,5′-tetramethyl stilbene (**III**)*

To a four-neck round-bottom flask equipped with a nitrogen inlet, heating mantle, stirrer, thermocouple and dean-stark trap, and temperature controller, 53 g of **II**, 451.2 g of DMSO and 370 g of epichlorohydrin were added. The reaction mixture was controlled at 65 °C, 15 mmHg and 33.4 g of 48 wt% $NaOH_{(aq)}$ was added gradually in 2 h and then the mixture was reacted at the temperature for 5 h. After the reaction was completed, the salt was filtered then the filtrate after water wash to remove trace salt was concentrated. Methanol (500 ml) was added into concentrated solution and stirred at room temperature. The precipitate epoxy was filtered and dried in an oven. IR absorption at 915 cm^{-1} (epoxy ring), 856 cm^{-1} (aromatic, C–H), 959 cm^{-1} (*trans*, Ar-HC=CH-Ar), 2921 cm^{-1} ($-CH_3$). The reaction equation was shown in Scheme 1.

*3.4. Synthesis of 4,4′-dihydroxy-3,3′,5,5′-tetramethyl-α-methyl stilbene (**IV**) [13]*

To a four-neck round-bottom flask equipped with a nitrogen inlet, heating mantle, stirrer, thermocouple and temperature controller, 61 g (0.5 mol) of 2,6-dimethyl phenol and 23.13 g of chloroacetone were added. The reaction mixture was gradually cooled to 0 °C and then 24.5 g of H_2SO_4 was added gradually for 2 h. After that, the reaction mixture was maintained at room temperature for another 2 h. After the reaction was completed, the reaction solution was poured into ice water to remove excess H_2SO_4. The precipitate was recrystallized from H_2O/ethanol (1/1) mixture twice. Elemental analyses for $C_{19}H_{22}O_2$: C = 80.85%, H = 7.80%, O = 11.35% (theoretically) and C = 80.81%, H = 7.76%, O = 11.43% (experimentally). IR absorption at 840 cm^{-1} (Ar–CC=CH–Ar), 868 cm^{-1} (aromatic, C–H), 2969 cm^{-1} ($-CH_3$) and 3103–3605 cm^{-1} (–OH). The reaction equation was shown in Scheme 1.

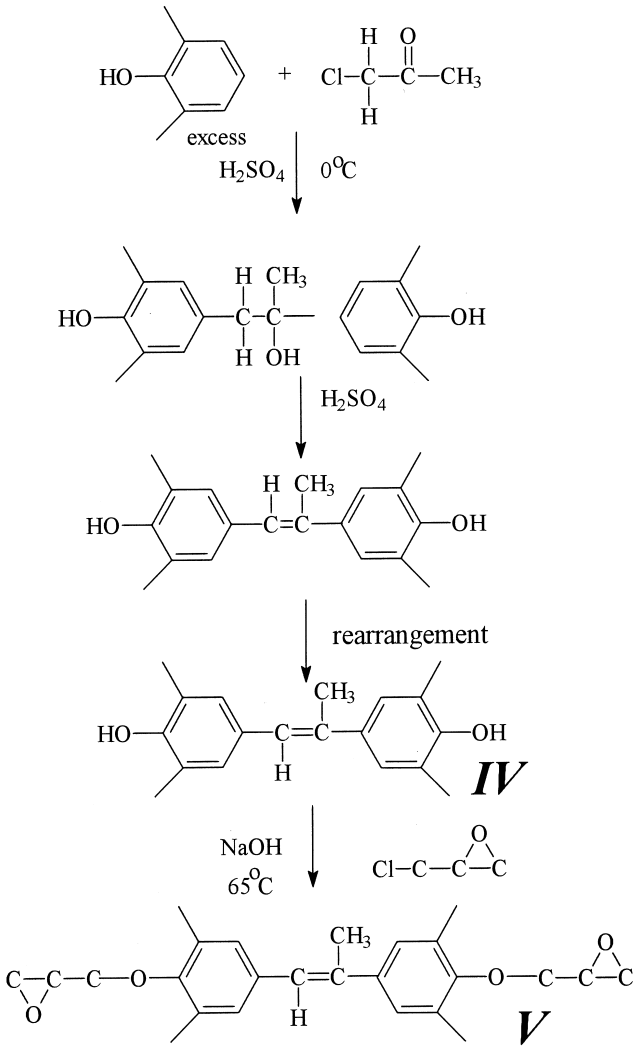

Scheme 2. The reaction equation and structure of **IV** and **V**.

*3.5. Synthesis of 4,4′-bis(2,3-epoxypropoxy)3,3′,5,5′-tetramethyl-α-methyl stilbene (**V**)*

To a four-neck round-bottom flask equipped with a nitrogen inlet, heating mantle, stirrer, thermocouple and temperature controller, 56.4 g (0.2 mol) of **IV**, 74 g of DMSO and 370 g of epichlorohydrin were added. The reaction mixture was controlled at 65 °C, 15 mmHg and 33.4 g of 48 wt% $NaOH_{(aq)}$ was added gradually for 2 h and then the mixture was reacted at that temperature for 5 h. After the reaction was completed the salt was filtered, then the filtrate was washed with water for three times. The organic phase was separated. The excess epichlorohydrin and solvent was distilled by a rotary and **V** was obtained. The reaction equation was shown in Scheme 2.

4. Curing procedure

III, **V** and TMBP epoxy were cured with DDM and DDS,

respectively. The reactant compositions were mixed in a 1:1 equivalent ratio. The mixture was crushed into fine powder and then heated on a hot plate at about 150 °C with continuous stirring until a homogeneous solution was obtained. For DDM curing system, the mixtures were cured at 180 °C for 2 h, 200 °C for 2 h and 215 °C for 2 h. For DDS curing system, the mixtures were cured at 210 °C for 2 h, 230 °C for 2 h and 260 °C for 2 h. After that, samples were allowed to cool slowly to room temperature in order to prevent cracking.

5. Result and discussion

*5.1. Characterization of 1,1-bis(4-hydroxy-3,5-dimethylphenyl)-2-chloroethane (**I**)*

I was synthesized from the nucleophilic substitution of chloroacetaldehyde dimethylacetal and 2,6-dimethyl phenol in the acid condition. As shown in Scheme 3, chloroacetaldehyde dimethylacetal reacted with H^- in the first step, then 2,6-dimethyl phenol attacks the carbon of activated intermediate and methanol was released to obtain **I** in the second step. To avoid 2,6-dimethyl phenol attack at the chlorine of activated intermediate, the reaction temperature was maintained at 5 °C. The melting point of **I** was in the range 165–166 °C, which implies that the purity of **I** was very high due to its small melting range. Fig. 1(a) and (b) shows ^{1}H-NMR and ^{13}C-NMR spectra of **I**, respectively.

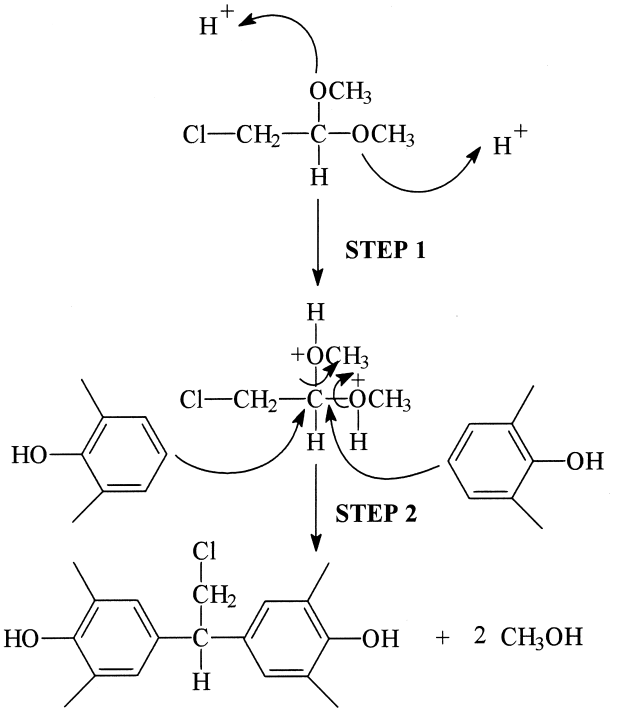

Scheme 3. The mechanism of nucleophilic substitution of chloroacetaldehyde dimethylacetal and 2,6-dimethyl phenol in the acid condition.

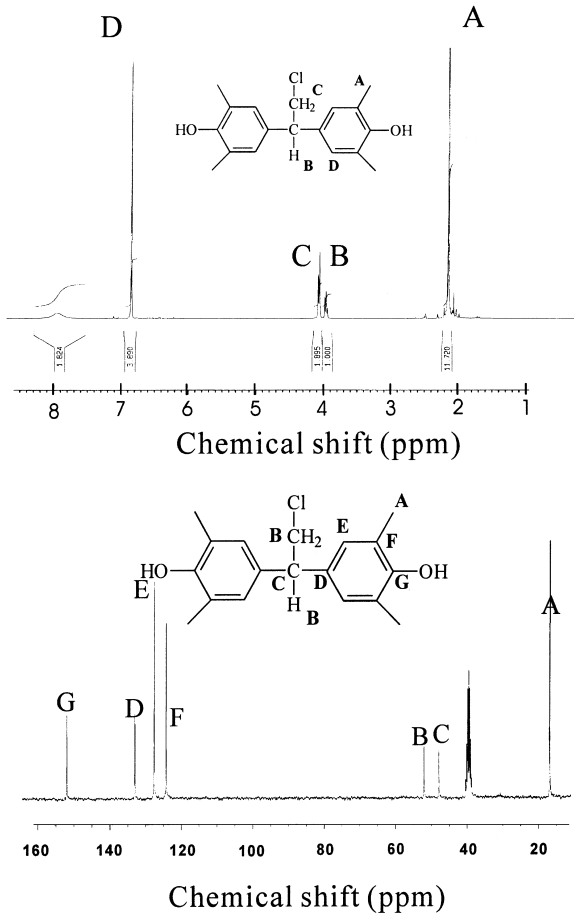

Fig. 1. (a) ^{1}H-NMR and (b) ^{13}C-NMR spectra of **I**.

From ^{1}H-NMR, one can see the characteristic chemical shift at δ(ppm) = 6.85 (s, 4H, aromatic), 4.08 (d, 2H, CH_2Cl), 3.98 (m, 1H, –CH–) and 2.15 (s, 12H, CH_3). From ^{13}C-NMR, one can see the characteristic chemical shift at δ(ppm) = 152.05, 133.12, 127.69, 124.33, 52.16 (–CH_2Cl), 48.05 (–C–Cl–) and 17.01 (CH_3). Mass spectrum shows the characteristic peak at 304 cm^{-1} (M^+, base) and 255 cm^{-1} (M-CH_2Cl^+).

*5.2. Characterization of 4,4′-dihydroxy-3,3′,5,5′-tetramethyl stilbene (**II**)*

II was obtained from the de-hydrogen chloride of **I** in a base condition. According to the structure of **I**, the de-HCl should produce **I′** instead of **II**. However, all spectral analyses indicate product **II** was obtained which implies **I′** may rearrange into **II** due to **II** has less steric hindrance than **I′**. The rearrange mechanism of **I′** to **II** was difficult to define and describe. One possible rearrangement mechanism may be as follows.

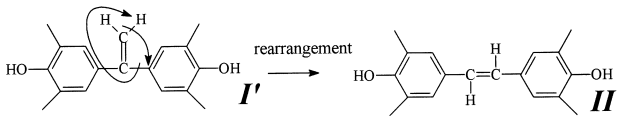

The melting point of **II** was in the range 248–250 °C, which implies that the purity of **II** was high due to its small melting range. Fig. 2(a) and (b) shows ^{1}H-NMR and ^{13}C-NMR spectra of **II**, respectively. From ^{1}H-NMR, one can see the characteristic chemical shift at δ(ppm) = 7.08 (s, 4H, aromatic), 6.82 (s, 2H, Ar-HC=CH-Ar) and 2.18 (s, 12H, $-CH_3$). The ratio of integral area for chemical shift at 7.08, 6.82 and 2.18 is 2:1:6, which is consistent with the structure of **II**. From ^{13}C-NMR, one can see the characteristic chemical shift at δ(ppm) = 152.94, 128.9, 126.4, 125.53 (Ar-HC=CH-Ar), 124.56 and 15.92 ($-CH_3$). Fig. 2(c) shows the DEPT 135 spectrum of **II**. If product **I′** is obtained, it should contain four tetra-carbon. However, as shown in Fig. 2(c), only three tetra-carbon was observed, which is consistent with the structure of **II**. Mass spectrum shows the characteristic peak at 268 cm^{-1} (M^+, base), 238 cm^{-1} (M-2 CH_3^+) and 134 cm^{-1}. The characteristic peak at 134 cm^{-1}, derived from breaking of C=C, strongly implies the symmetry of the product. It indicated that the product **II**, not **I′**, was obtained. From IR spectrum, the characteristic peak at 948 cm^{-1} is the *trans* absorption of –HC=CH–.

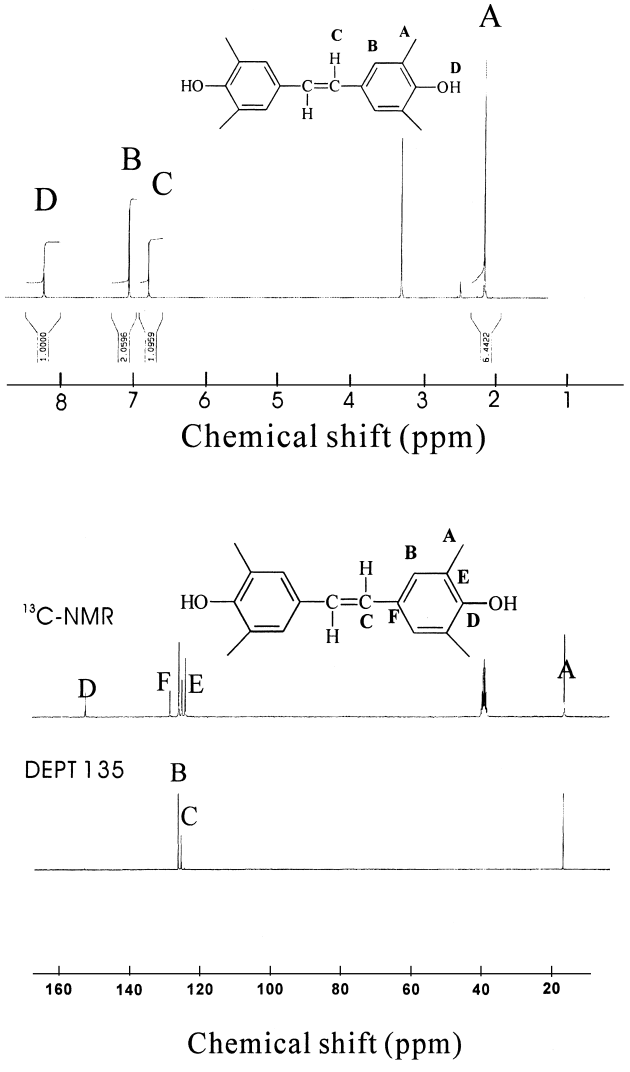

Fig. 2. (a) ^{1}H-NMR and (b) ^{13}C-NMR (c) DEPT 135 spectra of **II**.

5.3. Characterization of 4,4′-bis(2,3-epoxypropoxy)-3,3′,5,5′-tetramethyl stilbene (*III*)

The melting point of **III** was in the range 150–153 °C, which is much lower than that of **II**. Fig. 3 shows ^{1}H-NMR spectrum of **III**. From ^{1}H-NMR, one can see the characteristic chemical shift at δ(ppm) = 7.21 (s, 4H, aromatic), 6.97 (s, 2H, (Ar-HC=CH-Ar)), 3.35–4.09 (m, 4H), 3.33 (m, 1H), 2.26–2.82 (m, 4H, CH_3) and 2.22 (s, 12H). The peak at 2.64–4.09 ppm is the characteristic peak of oxirane. Fig. 4 shows the mass spectrum of **III**. The characteristic peak at 380 cm^{-1} (M^+, base), 323 cm^{-1} (M-87$^+$) and 267 cm^{-1} (M-174$^+$) were observed. According to the titration of EEW, its EEW value is 192 g/equiv., which is close to the theoretical value of 190 g/equiv.

5.4. Characterization of 4,4′-dihydroxy-3,3′,5,5′-tetramethyl-α-methyl stilbene (*IV*)

IV was synthesized from the nucleophilic substitution and addition of chloroacetone and 2,6-dimethyl phenol in the acid condition. As shown in Scheme 4, chloroacetone reacted with H^+, and then 2,6-dimethyl phenols attack the carbon of activated intermediate by nucleophilic substitution and addition process. The intermediate was dehydrated and rearranged to obtain **IV**. The melting point of **IV** was in the range 170–171 °C, which implies that the purity of **IV** was very high due to its small melting range. Fig. 5 shows ^{1}H-NMR spectrum of **IV**. From ^{1}H-NMR, one can see the characteristic chemical shift at δ(ppm) = 7.06 (s, 2H, aromatic), 6.90 (s, 2H, aromatic), 6.57 (s, 1H, Ar-RC=CH-Ar), 2.17 (d, 12H, Ar-CH_3) and

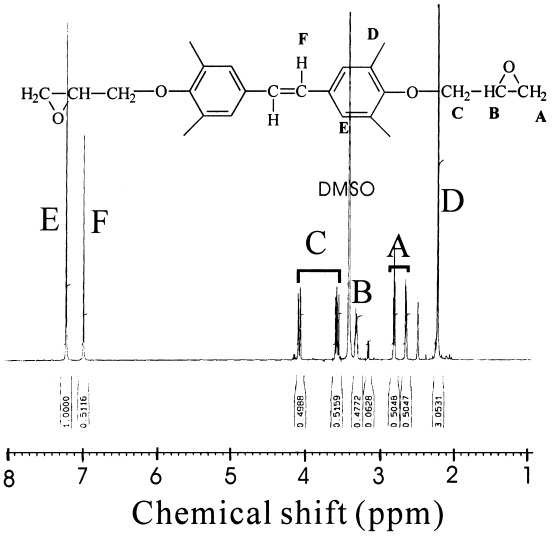

Fig. 3. ^{1}H-NMR spectrum of **III**.

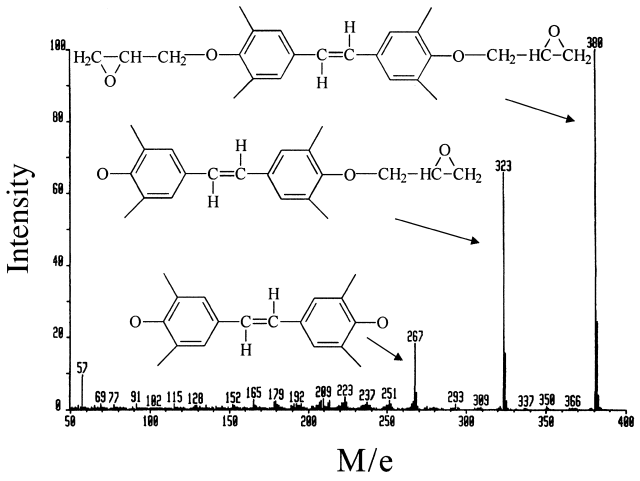

Fig. 4. Mass spectrum of **III**.

2.12 (s, 3H, C=C(CH_3)-Ar). Mass spectrum shows the characteristic peak at 282 cm^{-1} (M^+, base). From IR spectrum, the characteristic peak at 840 cm^{-1} is shown for Ar-CC=CH-Ar).

*5.5. Characterization of 4,4′-bis(2,3-epoxypropoxy)-3,3′,5,5′-tetramethyl-α-methyl stilbene (**V**)*

From IR spectrum, **V** shows characteristic absorption at 839 cm^{-1} (Ar-CC=CH-Ar), 856 cm^{-1} (aromatic, C–H), 915 cm^{-1} (epoxy ring), 1215 cm^{-1} (Ar–O–C) and 2919 cm^{-1} (–CH_3). Its EEW is 207 g/equiv., which is closer to the theoretical value of 197 g/equiv.

6. Thermal properties of cured epoxy resins

6.1. DSC scans

According to dynamic DSC scans of **III**, **V** and commercial TMBP epoxy cured with DDM and DDS, their exothermic temperatures are in the range 160–220 and 230–275 °C, respectively. A curing agent exhibiting a lower exothermic starting temperature under the same set of curing condition is more reactive toward the epoxy resins. It is therefore reasonable to propose that the chemical reactivity of these two curing agents toward the epoxy resin is DDS < DDM due to the sulfone group in DDS is a strong electron withdrawing group both by induction (-I) and mesomeric (-M) effects. However, no obvious difference in exothermic temperature was observed among these three epoxy resins.

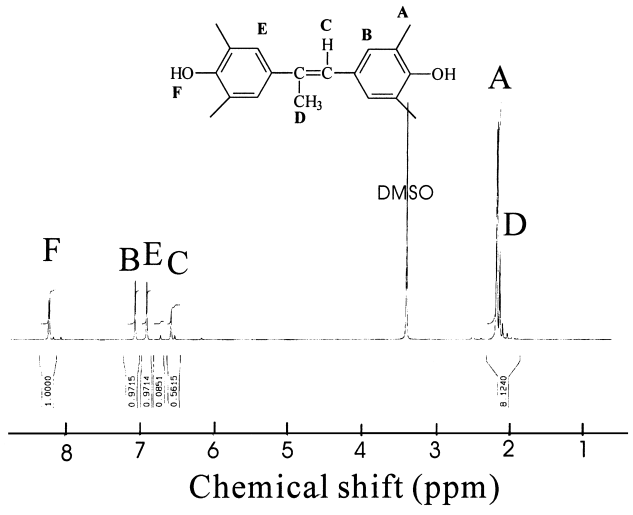

Fig. 5. ^{1}H-NMR spectrum of **IV**.

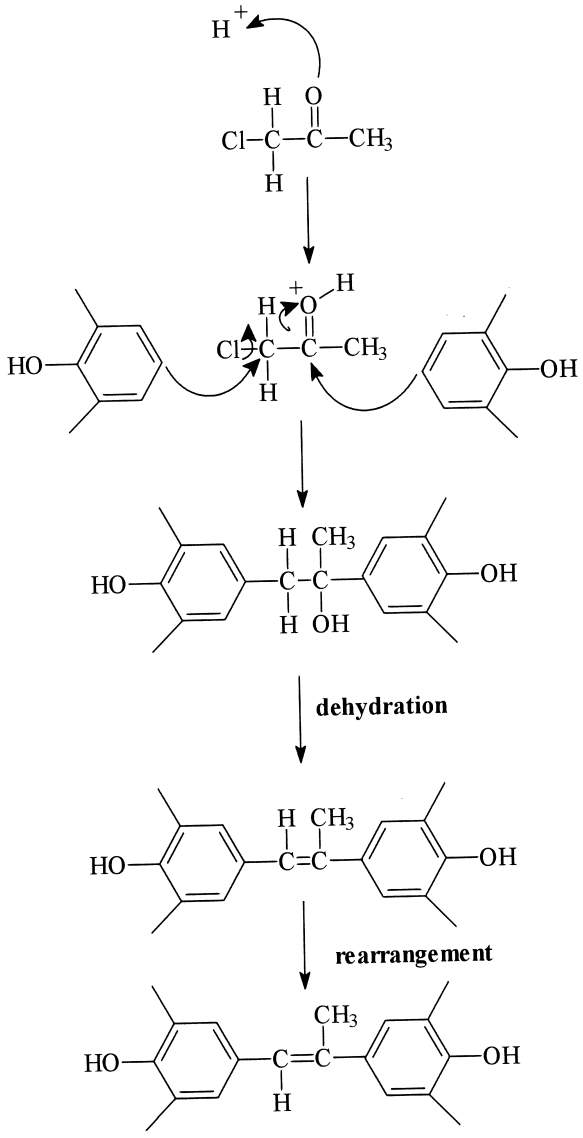

Scheme 4. The formation mechanism of **IV**. Step 1: nucleophilic substitution and addition of 2,6-dimethyl phenol and chloroacetone in the acid condition. Step 2: dehydration and rearrangement of intermediate product to get **IV**.

6.2. Curing kinetics: dynamic method I (Kissinger's method [14])

The data from dynamic DSC measurements are analyzed by Eq. (1)

$$r = \frac{dx}{dt} = \beta\frac{dx}{dT} = A\,e^{-E/RT}(1-x)^n \quad (1)$$

where x is the conversion, t the time, T the temperature, β the heating rate and $T = T_0 + \beta t$. Since the maximum rate takes place when dx/dt is zero, differential equation of (1) with respect to time and equating the resulted expression with zero gives Eq. (2):

$$\beta\frac{E}{RT_p^2} = An(1-x)p^{n-1}\,e^{-E/RT_p} \quad (2)$$

where T_p is the maximum rate temperature. Eq. (2) can be written in the natural logarithm form shown in Eq. (3):

$$-\ln\left(\frac{\beta}{T_p^2}\right) = \ln\left(\frac{E}{R}\right) - \ln(An) - (n-1)\ln(1-x)_p + \frac{E}{RT_p} \quad (3)$$

The above expression yields linear plot of $-\ln(\beta/T_p^2)$ against $(1/T_p)$, and the activation energy can be obtained from the slope of the corresponding straight line. The activation energy calculated according to the plot of $-\ln(\beta/T_p^2)$ against $(1/T_p)$ (not shown here briefly) are 49.96, 48.28 and 45.16 kJ/mol for **III**/DDM, **V**/DDM and TMBP/DDM, respectively, and 62.56, 60.39 and 57.03 kJ/mol for **III**/DDS, **V**/DDS and TMBP/DDS, respectively.

6.3. Curing kinetics: dynamic method II (Ozawa's method [15])

Another theoretical treatment, namely the Ozawa's method can also be applied to the thermal data. He reported Eq. (4):

$$\log\beta = \frac{1}{2.303}\ln\beta = -0.4567\frac{E}{RT} + \left(\log\frac{AE}{R} - \log F(x) - 2.315\right) \quad (4)$$

where β is the heating rate, E the activation energy, R the ideal gas constant and $F(X)$ the conversion-dependent term.

Thus, at the same conversion, a plot of $\ln(\beta)$ versus $1/T_p$ should be a straight line with a slope of $(2.303 \times 0.4567)E/R$. The activation energy calculated from the plot of $\ln(\beta)$ versus $1/T_p$ (not shown here briefly) are 54.86, 53.49 and 50.15 kJ/mol for **III**/DDM, **V**/DDM and TMBP/DDM, respectively, and 67.71, 65.61 and 62.43 kJ/mol for **III**/DDS, **V**/DDS and TMBP/DDS, respectively.

According to the results described above, epoxy resins **III** and **V** exhibit similar activation energy compared with commercial TMBP epoxy resin.

6.4. DMA measurement

Table 1 shows DMA data of cured **III**, **V** and TMBP epoxy system. Their T_g's (peak temperature of loss tangent) for DDM-cured system are 222, 193 and 210 °C, respectively. The heights of loss tangent are 0.104, 0.129 and 0.136, separately. The storage moduli at 50 °C are 1.64, 1.89 and 2.16×10^9 Pa; and at $T_g + 40$ °C are 2.54, 2.21 and 1.87×10^8 Pa, individually. The order of T_g for cured epoxy system is **III** > TMBP > **V**. Fig. 6 shows minimum energy molecular structure (calculated by CS chem3D pro) **III**, TMBP and **V**. According to Fig. 6, ph-HC=CH-ph in **III** is a co-plane structure, and thus has highest packing density, therefore, lowest free volume. However, the bulky methyl group has made ph-(CH_3)C=CH-ph in **V** is not a co-plane structure, and thus has the lowest packing density, therefore, highest free volume. Thus, **III**/DDM system exhibits highest T_g and **V**/DDM system has lowest T_g. Similar DMA results were observed in DDS curing systems and the results are shown in Table 1. According to DMA measurements, modulus of DDS curing system was lower than that of DDM curing system but higher glass transition temperature. From the view point of free volume theory, the phenomenon seems to be unreasonable based on the free volume theory. However, factors that influence glass transition temperature including free volume, structure, intermolecular interaction, cross-link density and so on. The higher intermolecular interaction of the sulfone group in DDS-cured resins resulted in higher glass transition temperature than that of DDM-cured resins. While the lower modulus in the rubbery regions for the DDS-cured resins than that of the

Table 1
DMA data of cured **III**, **V** and TMBP epoxy system

Sample ID	T_g (°C)	tan δ	Modulus, 50 °C (GPa)	Modulus, $T_g + 40$ °C ($\times 10^8$ Pa)
TMBP/DDM	210	0.136	2.16	1.870
III/DDM	222	0.104	1.84	2.540
V/DDM	193	0.129	1.89	2.210
TMBP/DDS	239	0.267	2.39	0.611
III/DDS	269	0.283	2.32	0.797
V/DDS	225	0.294	1.95	0.803

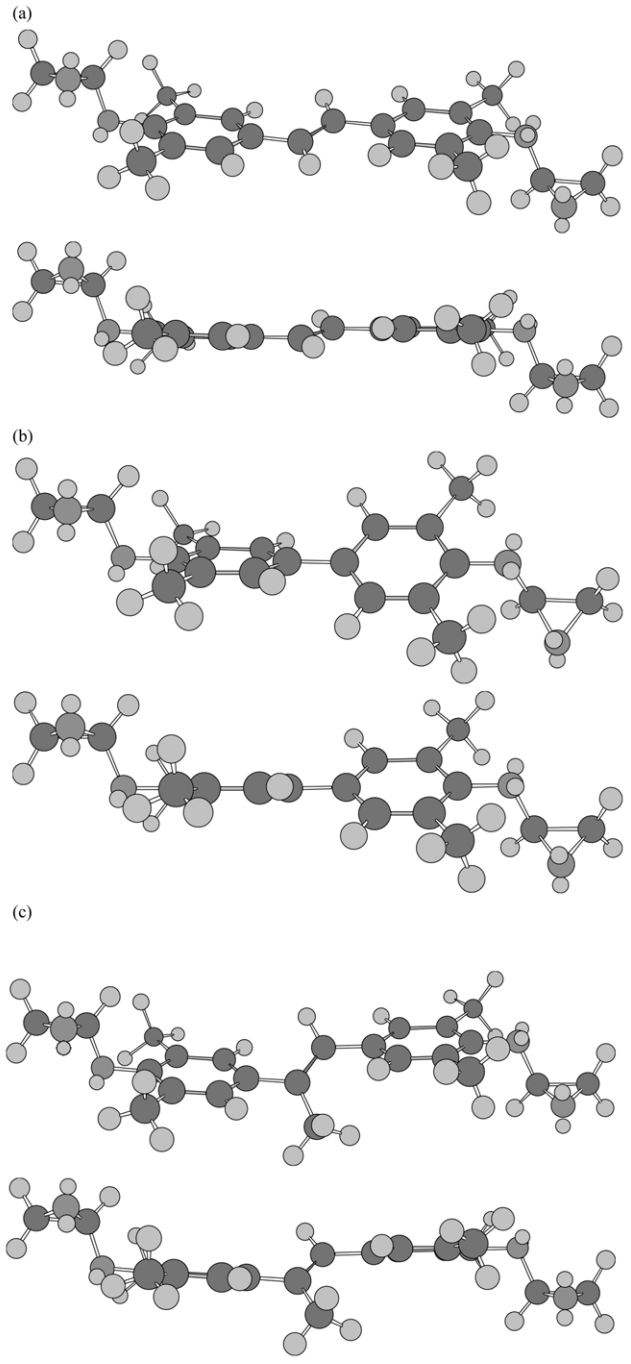

Fig. 6. Minimum energy molecular structure (calculated by CS chem3D pro) of: (a) **III**; (b) TMBP; (c) **V**. The dark balls are carbon, the off-black balls are oxygen, the grey balls are hydrogen and the small white balls are lone-pair electrons of oxygen.

DDM-cured resins may be due to lower cross-link density of the DDS-cured system because of the lower reactivity of DDS than DDM.

6.5. Moisture absorption

Moisture absorption will reduce the glass transition temperature of encapsulating material and may cause 'popcorn effect' when meeting with solder at high temperature. Moisture absorption will also ionize the ionic impurities (e.g. Cl^-) and thus corrode the integrated circuits. Furthermore, moisture absorption will increase encapsulating material's dielectric constant. Thus, lower moisture absorption is good for encapsulating materials. From Table 2, the order of moisture absorption for cured epoxy system is **V** < **III** < TMBP. The lowest moisture absorption may be attributed to more moisture repulsive methyl group (five CH_3) than that of **III** and TMBP (four CH_3). As to the **III** and TMBP system, it may be attributed to **III** has lower free volume than that of TMBP.

Table 2
Moisture absorption of cured **III**, **V** and TMBP epoxy system

Sample ID	Moisture absorption (%)	Sample ID	Moisture absorption (%)
TMBP/DDM	2.4	TMBP/DDS	2.9
III/DDM	2.3	**III**/DDS	2.5
V/DDM	2.2	**V**/DDS	2.3

6.6. TGA analysis

TGA traces of cured epoxy provided additional information regarding their thermal stability and thermal degradation behavior. TGA results of cured epoxy were shown in Table 3. In the nitrogen atmosphere, the 5% degradation temperature for DDM curing system was in the range 370–377 and 397–412 °C for DDS curing system. In the air atmosphere, the 5% degradation temperature for DDM curing system was in the range 372–385 and 410–411 °C for DDS curing system. No obvious tendency was observed for these curing systems. However, the 5% degradation temperature is lower than common epoxy [such as DGEBA/DDM ($5\%T_d = 411$ °C (nitrogen), 412 °C (air)), and DGEBA/DDS ($5\%T_d = 428$ °C (nitrogen), 415 °C (air))] due to the methyl group has low thermal stability.

6.7. TMA analysis

There are two major reasons which cause failure of electronic encapsulation. One is water absorption and the other is internal stress [16]. Thus, to increase the reliability of

Table 3
TGA results of cured **III**, **V** and TMBP epoxy system

Sample ID	5% T_d (°C)		Char yield at 800 °C	
	N_2	Air	N_2	Air
TMBP/DDM	375.28	372.58	11.31	1.36
III/DDM	377.15	377.81	18.41	4.21
V/DDM	370.3	385.16	21.37	7.01
TMBP/DDS	404.25	411.36	14.17	0
III/DDS	412.80	410.20	20.54	2.44
V/DDS	397.42	411.25	23.66	3.11

Table 4
TMA analysis of cured **III**, **V** and TMBP epoxy system

Sample ID	α ($\times 10^{-6}$/°C)[a]	α ($\times 10^{-6}$/°C)[b]
TMBP/DDS	57	182
III/DDS	53	175
V/DDS	62	189

[a] Average value was calculated between 50 and 100 °C.
[b] Average value was calculated between T_g + 50 and T_g + 100 °C.

encapsulation, moisture absorption and internal stress must be reduced. The internal stress may result from the difference in thermal expansion coefficient between silicon and encapsulation material. According to Table 4, the CTE of DDS curing system was in the range 53–62 ppm/°C. The CTE is in inverse order with T_g, therefore, **III**/DDS < TMBP/DDS < **V**/DDS. It implies that the higher free volume will cause higher thermal expansion.

7. Conclusions

The stilbene-based epoxy resins (**III** and **V**) were synthesized successfully by two steps from 2,6-dimethyl phenol and chloroacetaldehyde dimethylacetal or chloroacetone. The structures of these compounds have been confirmed by various instruments. According to NMR spectra, **I**′ will rearrange into **II** by an undetermined process. According to DMA, the order of T_g for cured epoxy system is **III** > TMBP > **V**. These may be attributed ph-HC=CH-ph in **III** is a co-planar structure, and thus has highest packing density. However, the bulky methyl group has made ph-(CH_3)C=CH-ph in **V** non-co-planar structure, and thus has the lowest packing density. Thus, **III**/DDM system exhibits highest T_g and **V**/DDM system has lowest T_g. According TMA, the CTE is in inverse order with T_g which is consistent with the packing density described above. According to TGA, they have similar thermal stability compared with commercial TMBP system. However, the 5% degradation temperature is lower than common bisphenol A epoxy due to the substituted methyl group has low thermal stability. The order of moisture absorption for cured epoxy system is **V** < **III** < TMBP. The lowest moisture absorption may be attributed to more moisture repulsive methyl group (five CH_3) than that of **III** and TMBP (four CH_3). As to the **III** and TMBP system, it may be attributed to **III** has lower free volume than that of TMBP. The combination of high T_g, outstanding resistance to moisture absorption and similar curing behavior as TMBP, make **III** and **V** attractive electronic encapsulation materials.

References

[1] Barclay CC, Ober CK, Papathomas KI, Wang DW. J Polym Sci, Polym Chem 1992;30:1831.
[2] Barclay CC, McNamee SG. J Polym Sci, Polym Chem 1992;30:1845.
[3] Lin Q, Yee AF, Jimmy DE, Sue HJ. Polymer 1994;35:2679.
[4] Broer DJ, Lub J. Macromolecules 1993;26:1244.
[5] Mallon JJ, Adams PM. J Polym Sci, Polym Chem 1993;31:2249.
[6] Shiraishi T, Motobe J, Ochi M, Nakanishi Y, Konishi T. Polymer 1992;33:2975.
[7] Ochi M, Yamashita K, Yoshizumi M, Shimbo M. J Appl Polym Sci 1989;38:789.
[8] Ochi M, Tsuyuno N, Sakaga K, Nakanishi Y, Murata Y. J Appl Polym Sci 1995;56:1161.
[9] Lin LL, Ho TH, Wang CS. Polymer 1997;38:1997.
[10] Lee MC, Ho TH, Wang CS. J Appl Polym Sci 1996;62:617.
[11] JP Kokai 8-73562, Sumitomo Chemical Company; 1996.
[12] JP Kokai 10-218972, Sumitomo Chemical Company; 1996.
[13] JP Kokai 10-298170, Sumitomo Chemical Company; 1996.
[14] Kissinger HE. Anal Chem 1957;29:1072.
[15] Ozawa T. Bull Chem Soc Jpn 1965;38:1881.
[16] Ho TH, Wang CS. Polymer 1996;37:2733.